Characterization of a water-based hybrid metal pretreatment coating

Danqing Zhu[1)1*], Naiping Hu[2)] Dale W. Schaefer[2)] and Peter Zarras[3)]
1) Ecosil Technologies LLC, Fairfield OH 45014
2) Department of Biomedical, Chemical and Environmental Engineering, University of Cincinnati, Cincinnati, Ohio 45221-0012
3) Naval Air Systems Command (NAVAIR), 1900 N. Knox Road, China Lake, CA 93555-6106

Abstract

A water-based hybrid pretreatment coating was characterized by SEM, AES and X-ray reflectivity (XRR) to obtain a comprehensive understanding on its coating structure and on the coating formation mechanism. The corresponding solution for forming this hybrid pretreatment coating consists of a waterborne silicon-containing oligomer and hexafluoroziconic acid. This pretreatment coating has demonstrated equal or better paint adhesion and anti-corrosion performance than traditional pretreatment coatings. SEM revealed that the coating morphology is characteristic of a rough texture due to uniform deposition of zirconium oxide nano-particles over the metal surface. AES result indicated that the pretreatment coating consists of a zirconium-rich region at the metal/coating interface while the coating surface is enriched with organic components containing high amounts of C and Si. XRR further elucidated that this hybrid pretreatment coating has two distinct sub-structures: a 5-nm thick ZrO_2-rich dense layer at the metal interface and a 20-nm thick organic-rich layer located on the top. This organic-rich top layer is dominated by a crosslinked silsesquioxane network with some embedded ZrO_2 nano-particles.

1. Introduction

Metal pretreatment coatings provide adhesion between paints and metal substrates for enhanced corrosion resistance of painted metal systems. Traditional pretreatments such as hexavalent chromium (Cr(VI)) conversion coatings and phosphate-based pretreatments have been widely-used for decades in coating industries[1-3], however, the use of these pretreatments has been regulated worldwide due to severe health and environmental concerns caused by their chemistries. Cr(VI) conversion coatings contains hexavalent chromium ions which are known as carcinogenetic [4, 5]. Chronic inhalation of Cr(VI) compounds increases the risk for lung cancer. Soluble species can cause or exacerbate contact dermatitis. Ingestion can cause irritation and ulcers of the stomach and intestine where Cr(VI) is transported into cells via the "sulfate transport" mechanism [6]. Phosphate-based pretreatments raise environmental concerns due to their impact on water sources. The discharge of phosphates into surface water results in "eutrophication," which causes rapid oxygen depletion in water due to excessive plant growth and decay. [7, 8] Eutrophication eventually kills fish and other aquatic organisms. Additionally, heavy metal ions such as nickel and cobalt in the zinc phosphate pretreatment formulas are toxic to humans.

---

[1] * Corresponding author Tel: +1 513-858-2365; Fax: +1 513-829-5387; Email: zhud@ecosiltech.com

Recent research and development efforts have resulted in a group of non-toxic, environmentally-compliant alternative pretreatments such as zirconium oxide-based and organo-functional silane-based pretreatments [9-18]. These pretreatment coatings, ranging from 10 nm to 1μm thick, are formed on a metal surface via a sol-gel process and have demonstrated in industrial settings to effectively promote paint adhesion for metal substrates. Nevertheless, their major drawbacks, as described as follows, have also been identified during industrial operations.

Flash rusting associated with carbon steels with zirconium oxide-based pretreatment. Carbon steels are prone to rapid corrosion, known as "flash rusting," that instantly occurs when metals are exposed to aqueous corrosive environments. Powdery flash rusts formed on the steel surface drastically reduce subsequent paint adhesion. A carbon steel surface treated with an acidic zirconium pretreatment solution is susceptible to "flash rusting" if the treated steel surface is not sufficiently rinsed by de-ionized (DI) water to remove free fluoride ions (F$^-$) from the surface. In some cases, even thorough water rinsing cannot completely solving flash-rusting issue. Because of this drawback, the zirconium oxide pretreatment coating is NOT considered for "dry-in-place" processes where no post rinse step is applied.

"Pickiness" of silane-pretreated metals on paint types. Organo-functional silane-based pretreatment solutions are less corrosive than zirconium pretreatment solutions. A crosslinked silane pretreatment coating can mitigate flash rusting of carbon steel to a certain extent. However, the major drawback of silane-based pretreatment coatings is that they are "picky" regarding the subsequently-applied paint type. Matching of organo-functional group(s) of the silane molecule(s) to the paint type is a must to ensure excellent paint adhesion. However, this stipulation is not practical.

A group of hybrid pretreatment coatings, such as SILSBOND coatings developed by Ecosil Technologies LLC, have thus emerged as a better solution to overcome the major drawbacks of the above pretreatments. The generic composition of a SILSBOND solution is a mixture of waterborne silicon-containing oligomer with hexafluoroziconic acid (H_2ZrF_6) as an additive. SILSBOND coatings have demonstrated not only improved paint adhesion to a broad range of paints but also mitigate flash rusting issue for carbon steel substrates.

The aim of this study is to obtain a comprehensive understanding on the SILSBOND hybrid coating structure by using a variety of characterization techniques. In particular, this article highlights on, (1) surface morphology observation of this pretreatment coating using Scanning Electron Microscopy (SEM), (2) coating composition analysis by Auger Electron Spectroscopy (AES), and (3) coating structure analysis by X-ray reflectivity (XRR). Coating formation mechanism is also discussed based on these characterization results. Accelerated corrosion test results for SILSBOND-treated metals under paints are reported.

2. Results and discussion

2.1. Surface morphology characterization of SILSBOND-treated cold-rolled steel by SEM

Figure 1 compares the morphologies of a polished cold rolled steel (CRS) surface before and after immersion in a 2% diluted SILSBOND solution. Before immersion, the polished CRS shows a smooth surface without features, as seen in Figure 1(a). After being immersed in the SILSBOND solution for 60 s and then being ambient dried, the CRS surface is "roughened", which is attributed to the uniform deposition of numerous nano-particles on CRS (Figure 1(b)). These nano-particles are in different sizes, ranging from a few nanometers to 30 nm. Bigger particles are likely to be formed by agglomeration of smaller particles. The composition of the nano-particles is presumably to be zirconium oxide. A study by S. Adhikari et al [23] also revealed a similar surface morphology of CRS deposited with a zirconium oxide pretreatment coating from a diluted H_2ZrF_6 solution. It is to note that SILSBOND is a hybrid pretreatment coating which contains both organic and inorganic components. However, SEM cannot clearly reveal the feature of the organic component in the pretreatment coating.
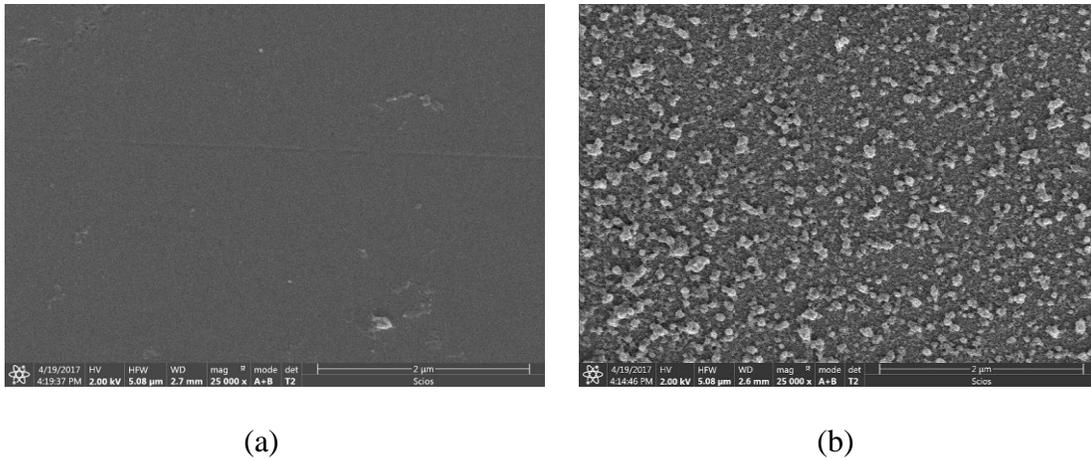

(a)   (b)

Figure 1. SEM images of a polished CRS surface before (a) and after (b) immersion in a SILSBOND pretreatment solution for 60s.

2.2. SILSBOND coating composition measured by AES

The composition of the SILSBOND hybrid pretreatment coating shown in Figure 1(b) was measured by AES. Table 1 shows the results for the surface composition of the hybrid pretreatment coating on CRS. A high amount of carbon (C), 35.6 at.%, is detected, indicating that the coating surface is enriched with organic components that is likely a crosslinked silsequioxane network.

Table 1. Surface composition of a hybrid pretreatment film deposited on CRS

Element, at.%						
Si	**Zr**	**C**	**N**	**O**	**F**	**Fe**
6.9 ± 0.5	7.0 ± 1.0	35.6 ± 0.9	5.6 ± 0.3	31.8 ± 0.2	11.2 ± 0.2	1.9 ± 0.6

Figure 2 shows the AES depth profile of the hybrid pretreatment coating on CRS. The distribution of the main elements was measured by AES through the cross-sections of the

pretreatment coating from the coating surface to the metal substrate. It is noticed that the contents of C and Si are the highest on the coating surface and then gradually decrease towards the metal substrate. The maximum contents of Zr and O are detected within the coating but not on the surface. This implies that the zirconium oxide nano-particles shown in Figure 1(b) are covered by a clear organic coating.
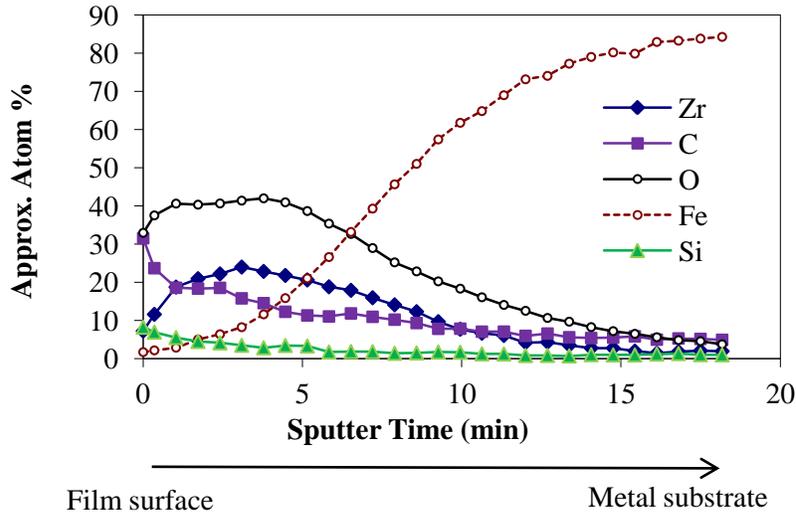
Figure 2. AES depth profiles of CRS deposited with a hybrid pretreatment coating

2.3. Coating structure elucidated by XRR (X-Ray Reflectivity)

The SILSBOND pretreatment coating structure was further characterized by XRR. In this study, a 100-nm Al layer was first deposited onto a Si wafer surface, and then the Al-coated Si wafer surface was immersed in a SILSBOND pretreatment solution for 30 s, followed by ambient drying. For a comparison purpose, another Al-coated Si wafer was immersed for 30 s in a SILSBOND solution without H_2ZrF_6. Figure 3 shows the XRR plots for the Al-coated Si wafer surfaces treated with the two SILSBOND solutions. It is seen in Figure 3(a) and 3(b) that before SILSBOND treatment ($t = 0$ s), the XRR curve for the Al-coated Si wafer surface exhibits two types of fringes: (1) closely-spaced fringes within the q range from 0.5 to 0.7 nm^{-1} which represents the 100-nm Al layer deposited on the Si wafer surface, and (2) a broad fringe in the range $0.7 < q < 1.5$ nm^{-1} which represents the naturally-formed aluminum oxide on the Al layer.

Figure 3(a) shows XRR curves for the Al surface before and after 30 s immersion in the SILSBOND solution without H_2ZrF_6. The fringes for the Al layer and the Al oxide remain unchanged after immersion. Figure 3(b) shows XRR curves for the Al surface before and after 30 s immersion in the H_2ZrF_6-containing SILSBOND solution. It is interesting to notice that the broad fringe for the Al oxide disappears and the closely-spaced fringes for the Al-layer are also greatly damped after immersion. This indicates that H_2ZrF_6-containing SILSBOND solution not only removes the Al oxide but also partially dissolves Al layer. This effect is likely due to the attack of F$^-$ ions in H_2ZrF_6 on the Al oxide and the Al substrate.
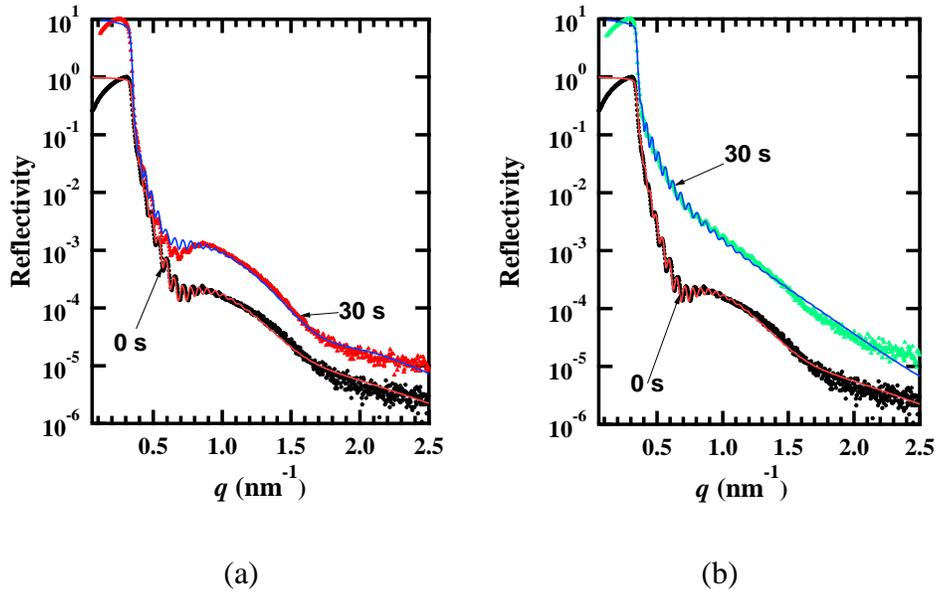
4

(a)   (b)

Figure 3. XRR plots for Al-coated Si wafers treated with (a) SILSBOND solution without H_2ZrF_6 and (b) SILSBOND solution with H_2ZrF_6 for 30 s followed by ambient drying

The XRR curves in Figure 3 were further interpreted by fitting the Reflectivity vs. q profiles with a 4-layer model [24] to extract information on the coating structures. The Parratt algorithm found in the Irena package [24] available from the Argonne National Laboratory was used to do the inversion. The fitted XRR spectra (i.e., the resulting SLD profiles) are shown in solid lines in Figure 4(a) and 4(b).
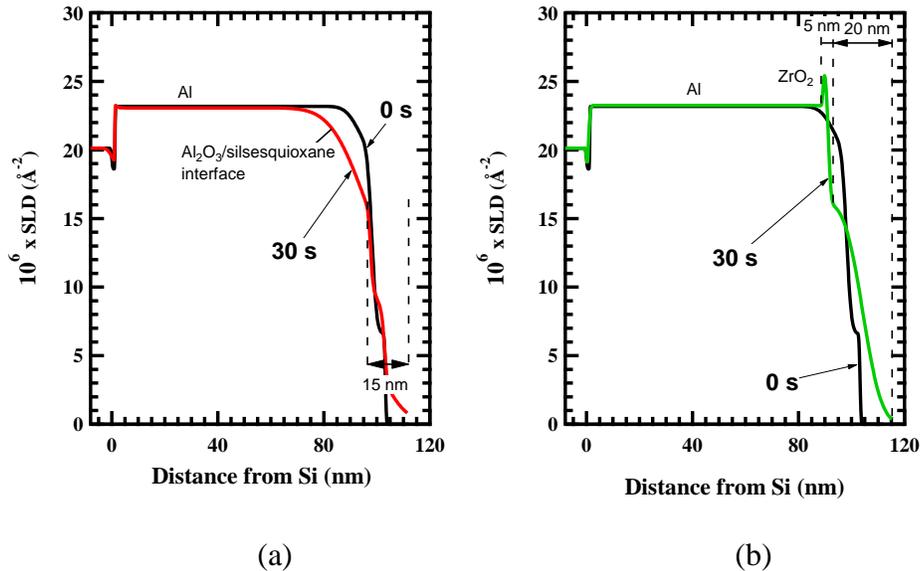

(a)   (b)

Figure 4. The fitting results presented as SLD profiles for Al-coated silicon wafers treated with (a) SILSBOND solution without H_2ZrF_6 and (b) SILSBOND solution with H_2ZrF_6 for 30 s followed by ambient drying

As is seen in Figure 4(a), after 30 s of immersion in the solution without H_2ZrF_6, an interfacial structure develops on top of the Al substrate. This interfacial structure has a lower SLD value than that of the native Al_2O_3 layer, and is likely to be a mixed region of a porous Al_2O_3 layer penetrated by a crosslinked silsequioxane network.

The SLD profile in Figure 4(b) for the pretreatment coating resulted from the H_2ZrF_6-containing solution reveals a different coating structure. It consists of two distinct sub-structures: a 5-nm thick layer at the Al interface with a high SLD value of 26.1×10^{-6} Å^{-2} and a 20-nm thick layer located on the top with much lower SLD values, $< 16.0 \times 10^{-6}$ Å^{-2}. Taking the SLD value of ZrO_2 (43.7×10^{-6} Å^{-2}) into consideration, the high SLD value of the interfacial layer is attributed to the formation of a layer enriched in ZrO_2 nano-particles. The top layer with lower SLD values is a mixed region consisting of less ZrO_2 and more organic component attributable to the silsesquioxane structure.

2.4. Discussion: the formation of the hybrid pretreatment coating on metal

Based on the above characterization results, mechanism for the formation of the hybrid pretreatment coating on metal is discussed. Figure 5 compares two types of pretreatment coating structures obtained from SILSBOND solutions with and without H_2ZrF_6, respectively.

When a metal is immersed in a SILSBOND solution without H_2ZrF_6, silsesquioxane molecules in the solution penetrate into pores in the oxide layer on the metal substrate. Upon drying, these silsesquioxane molecules crosslink to seal the pores and form a coating on top of the oxide layer, as is shown in Figure 5(a).

Figure 5(b) shows a different coating structure obtained from the SILSBOND solution (with H_2ZrF_6), which is characteristic of a ZrO_2-rich interfacial layer and an organic component (silsesequioxane)-rich top layer. Based on the characterization results, several distinct events may occur simultaneously on the metal surface upon coating formation. They are,

(1) the removal of the metal oxide layer and partial dissolution of the metal substrate due to the attack of F$^-$ ions from H_2ZrF_6, which is evidenced by XRR result shown in Figure 3(b),
(2) deposition of zirconium oxide nanoparticles on the oxide-free metal surface, which is revealed by SEM shown in Figure 3(b),
(3) penetration of silsesquioxane molecules into spaces between zirconium oxide nanoparticles and during the subsequent drying, the silsesquioxane molecules crosslink to seal the pores among zirconium oxide nanoparticles and form a dense coating on top of the zirconium oxide nano-particles, which is indicated by AES and XRR results.
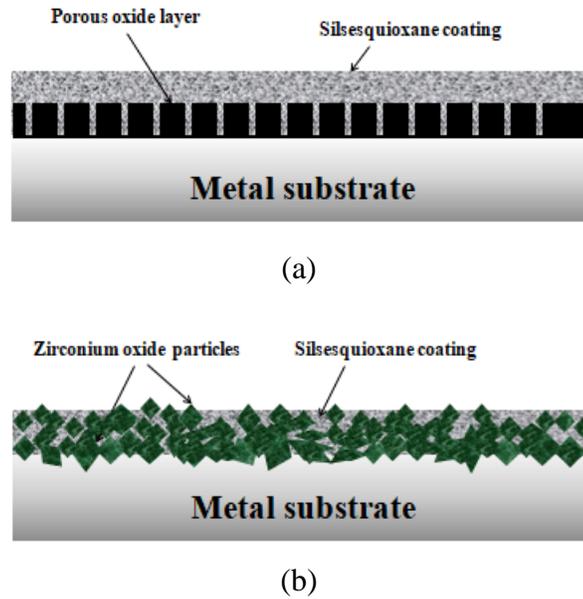
(a)

(b)

Figure 5. Schematic of the two types of pretreatment coating structures on a metal surface obtained from (a) SILSBOND solution without H_2ZrF_6, and (b) SILSBOND solution with H_2ZrF_6

The hybrid pretreatment coating structure in Figure 5(b) is advantageous over those of individual zirconium oxide-based and organo-functional silane based pretreatments, as it overcomes major drawbacks of these pretreatments. More specifically, a metal surface pretreated with a SILSBOND solution (with H_2ZrF_6) is activated or "cleaned" due to the etching effect of free F⁻ ions and is further roughened by the deposition of numerous zirconium oxide nano-particles. This ensures excellent adhesion to a broad range of paints. Simultaneously, a crosslinked silsesquioxane network forms to seal pores among zirconium oxide nano-particles. This dense top layer effectively prevents the ingress of moisture that is the main cause for flash rusting of carbon steels.

2.5. Corrosion protection performance of painted CRS and AA 2024-T3 pretreated with SILSBOND

Corrosion protection performance of the hybrid pretreatment coating was evaluated on CRS and AA 2024-T3 in accelerated corrosion tests. The test metal panels were primed with an epoxy primer (MIL-DTL-53022) and then coated with an aliphatic green polyurethane coat (MIL-DTL-53039). Figure 7 shows the coated CRS panels after 1022 hrs of salt spray test (in accordance with ASTM B117). The panel without pretreatment (Figure 6(a)) shows complete paint loss after the test, while the one with SILSBOND pretreatment (Figure 6(b)) exhibits much enhanced paint adhesion and corrosion protection.
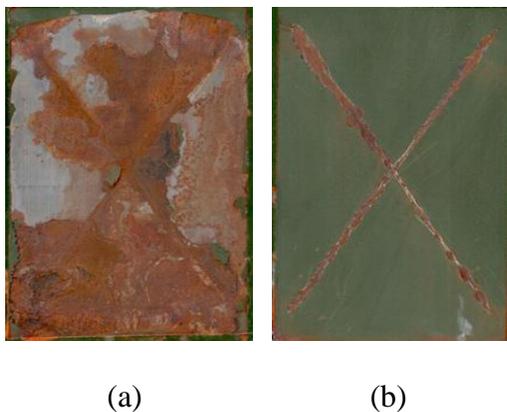
7

(a)   (b)

Figure 6. 1022 hr SST result for MIL-DTL-53022/ MIL-DTL-53039 coated CRS panels; (a) without pretreatment and (b) with SILSBOND pretreatment

Figure 7 displays the coated AA 2024-T3 panels after 30 cycles of GMW 14782 cyclic corrosion test. Before priming and topcoating, AA 2024-T3 panels were pretreated with a chromated wash primer and SILSBOND pretreatment, respectively. As is shown in Figure 8, both panels perform equally well.
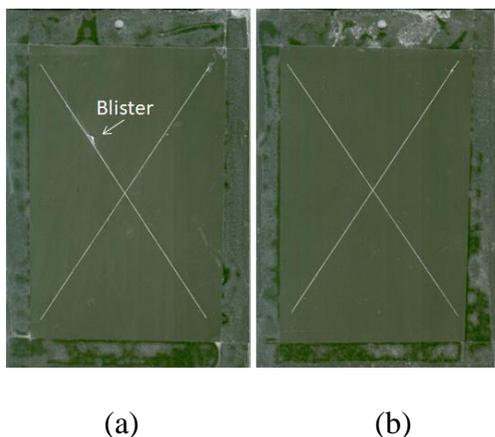

(a)   (b)

Figure 7. 30-cycle GMW 14782 cyclic corrosion test result for MIL-DTL-53022/ MIL-DTL-53039 coated Al 2024-T3; (a) pretreated with chromated wash primer (DOD-P-15328D) and (b) pretreated with SILSBOND

3. Conclusions

Zirconium oxide-based and organofunctional silane-based pretreatment coatings provide enhanced paint adhesion and corrosion protection for metal substrates, but they also have major drawbacks that have hindered them from widespread use. A group of hybrid pretreatment coatings have been developed, aiming to overcome these drawbacks.

A hybrid pretreatment coating, SILSBOND, developed by Ecosil Technologies was characterized using a variety of techniques. In general, it was found that the SILSBOND coating structure of SILBOND is advantageous over those of individual zirconium oxide-

based and organo-functional silane based pretreatments in terms of overcoming major drawbacks of these pretreatments. Important findings from this study are as follows:

- A metal surface pretreated with a SILSBOND solution (with H_2ZrF_6) is activated or "cleaned" due to the etching effect of free F^- ions and is further "roughened" by the deposition of numerous zirconium oxide nano-particles. This ensures excellent adhesion to a broad range of paints. Simultaneously, a crosslinked silsesquioxane network forms to seal pores among zirconium oxide nano-particles. This dense top layer effectively prevents the ingress of moisture that is the main cause for flash rusting of carbon steels.

- The coating consists of two distinct sub-structures: a 5-nm thick ZrO_2-rich dense layer at the metal interface and a 20-nm thick organic-rich layer located on the top. This organic-rich top layer is dominated by a crosslinked silsesquioxane network with some embedded ZrO_2 nano-particles.

Acknowledgements

References

[1] F.W. Eppensteiner, M.R. Jenkins, Chromate conversion coatings, Metal Finishing, 100, Supplement 1 (2002) 479-491.
[2] H.A. Katzman, G.M. Malouf, R. Bauer, G.W. Stupian, Corrosion-protective chromate coatings on aluminum, Appl. Surf. Sci., 2 (1979) 416-432.
[3] M. Kendig, S. Jeanjaquet, R. Addison, J. Waldrop, Role of hexavalent chromium in the inhibition of corrosion of aluminum alloys, Surf. Coat. Technol., 140 (2001) 58-66.
[4] E.P. Agency, National Emissions Standards for Chromium Emissions from Hard and Decorative Chromium Electroplating and Chromium Anodizing Tanks, in, Federal Register, RIN 2060-AC14, January, 1995.
[5] J. Blasiak, J. Kowalik, A comparison of the in vitro genotoxicity of tri- and hexavalent chromium, Mutat Res-Gen Tox En, 469 (2000) 135-145.
[6] K. Salnikow, A. Zhitkovich, Genetic and epigenetic mechanisms in metal carcinogenesis and cocarcinogenesis: Nickel, arsenic, and chromium, Chem. Res. Toxicol., 21 (2008) 28-44.
[7] M.C. Deyá, B. del Amo, E. Spinelli, R. Romagnoli, The assessment of a smart anticorrosive coating by the electrochemical noise technique, Prog. Org. Coat., 76 (2013) 525-532.
[8] P. Droniou, W.E. Fristad, J.-L. Liang, Nanoceramic-based conversion coating: Ecological and economic benefits position process as a viable alternative to phosphating systems, Metal Finishing, 103 (2005) 41-43.
[9] S.J. Elizabeth, G.H. Bruce, Zirconium-based coating compositions and processes. , in: United States Patent Application 20140227514, 2014.
[10] J. Ouyang, US Patent No. 5,662,967. 1997
[11] T. Matsuda, A. Matsuzaki, M. Sasaki, K. Takashima, US 2012/0088122 A1, 2012

[12] M. Yujiro, T. Akira, M. Atsushi, Patent No. JP2004197179, 2004

[13] T. Kolberg, M. Walter, P. Schubach, US patent no: 8101014 B2, 2012

[14] L. Fedrizzi, F.J. Rodriguez, S. Rossi, F. Deflorian, R. Di Maggio, The use of electrochemical techniques to study the corrosion behaviour of organic coatings on steel pretreated with sol-gel zirconia films, Electrochim. Acta, 46 (2001) 3715-3724.

[15] B. Schneider, A. Drews, M. Jagner, S. Simko, Characterization of Zirconium Oxide-Based Pretreatment Coatings Part 2 – Challenges in Coating Aluminum Body Panels, SAE Int. J. Mater. Manf., 2 (2009) 425-433.

[16] D. Zhu, W.J. van Ooij, Corrosion protection of AA 2024-T3 by bis-[3-(triethoxysilyl)propyl]tetrasulfide in sodium chloride solution.: Part 2: mechanism for corrosion protection, Corros. Sci., 45 (2003) 2177-2197.

[17] D. Zhu, W.J. van Ooij, Corrosion protection of AA 2024-T3 by bis-[3-(triethoxysilyl)propyl]tetrasulfide in neutral sodium chloride solution. Part 1: corrosion of AA 2024-T3, Corros. Sci., 45 (2003) 2163-2175.

[18] D. Zhu, W.J. van Ooij, Enhanced corrosion resistance of AA 2024-T3 and hot-dip galvanized steel using a mixture of bis-[triethoxysilylpropyl]tetrasulfide and bis-[trimethoxysilylpropyl]amine, Electrochim. Acta, 49 (2004) 1113-1125.

[19] X.C. Dong, P. Wang, S. Argekar, D.W. Schaefer, Structure and Composition of Trivalent Chromium Process (TCP) Films on Al Alloy, Langmuir, 26 (2010) 10833-10841.

[20] N.P. Hu, X.C. Dong, X.Y. He, S. Argekar, Y. Zhang, J.F. Browning, D.W. Schaefer, Interfacial morphology of low-voltage anodic aluminium oxide, J. Appl. Crystallogr., 46 (2013) 1386-1396.

[21] N.P. Hu, X.C. Dong, X.Y. He, J.F. Browning, D.W. Schaefer, Effect of sealing on the morphology of anodized aluminum oxide, Corros. Sci., 97 (2015) 17-24.

[22] G. Pan, E. Watkins, J. Majewski, D.W. Schaefer, Effect of thickness on the water-barrier properties of silane films, J Phys Chem C, 111 (2007) 15325-15330.

[23] S. Adhikaria, K.A. Unocica, Y. Zhaia, G.S. Frankela, J. Zimmermanb, W. Fristadb, Electrochimica Acta 56 (2011) 1912.

[24] J. Ilavsky, P.R. Jemian, Irena: tool suite for modeling and analysis of small-angle scattering, J. Appl. Crystallogr., 42 (2009) 347-353.